CANCER BIOTHERAPY AND RADIOPHARMACEUTICALS
Volume 33, Number 3, 2018

DOI: 10.1089/cbr.2017.2376

Original Articles

CLR 125 Auger Electrons for the Targeted Radiotherapy of Triple-Negative Breast Cancer

Joseph Grudzinski,[1] Ian Marsh,[1] Benjamin Titz,[2] Justin Jeffery,[3] Marc Longino,[2] Kevin Kozak,[2] Kristofer Lange,[2] Jason Larrabee,[2] Ashley Weichmann,[3] Amy Moser,[3,4] and Bryan Bednarz[1,3,4]

Abstract

Purpose: Auger electrons emitted by radioisotopes such as ^{125}I have a high linear energy transfer and short mean-free path in tissue (<10 μm), making them suitable for treating micrometastases while sparing normal tissues. The authors developed and subsequently investigated a cancer cell-selective small molecule phospholipid ether analog to deliver ^{125}I to triple-negative breast cancer (TNBC) cells *in vivo*.
Methods: A Current Good Manufacturing Practice (cGMP) method to radiolabel ^{125}I-CLR1404 (CLR 125) with >95% radiochemical purity was established. To estimate CLR 125 *in vivo* dosimetry and identify dose-limiting organs, the biodistribution of the analog compound ^{124}I-CLR1404 (CLR 124) was investigated using micro-positron emission tomography (PET)/computed tomography (CT) in conjunction with a Monte Carlo dosimetry platform to estimate CLR 125 dosimetry. *In vivo* antitumor efficacy was tested by injecting nude mice bearing either MDA-MB-231-luc orthotopic xenografts or lung metastases with 74 MBq (3.7 GBq/kg) of CLR 125 or an equivalent mass amount of nonradiolabeled CLR 125. Longitudinal tumor measurements using calipers and bioluminescence imaging were obtained for the xenografts and lung metastases, respectively.
Results: Dosimetry analysis estimated that CLR 125 would impart the largest absorbed dose to the tumor per injected activity (0.261 ± 0.023 Gy/MBq) while the bone marrow, which is generally the dose-limiting organ for CLR1404, appears to have the lowest (0.063 ± 0.005 Gy/MBq). At administered activities of up to 74 MBq (3.7 GBq/kg), mice did not experience signs of toxicity. In addition, a single dose of CLR 125 reduced the volume of orthotopic primary TNBC xenografts by $\sim$60% compared to control vehicle ($p < 0.001$) and significantly extended survival. In addition, CLR 125 was efficacious against preclinical metastatic TNBC models by inhibiting the progression of micrometastases ($p < 0.01$).
Conclusions: Targeted radionuclide therapy with CLR 125 displayed significant antitumor efficacy *in vivo*, suggesting promise for treatment of TNBC micrometastases.

Keywords: Auger electrons, CLR1404, targeted radionuclide therapy, theranostics, triple-negative breast cancer

Background

Breast cancer is the most common noncutaneous solid tumor in women worldwide, comprising 22.9% of all invasive cancers.[1] In the United States, over 230,000 new cases of breast cancer are diagnosed each year. Approximately 15%–20% of all cases are considered ''triple-negative'' breast cancer (TNBC) due to a lack of estrogen receptor (ER–), progesterone receptor (PR–), and human epidermal growth factor receptor 2 (HER-2–) protein expression, all of which serve as major targets for targeted therapies. The incidence of TNBC is higher in young minority women who face worse prognosis (both higher rates of early recurrence and death from their disease) than other ethnic groups.[2,3] Even when clinically

[1]Department of Medical Physics, University of Wisconsin–Madison, Madison, Wisconsin.
[2]Cellectar Biosciences, Inc., Madison, Wisconsin.
[3]University of Wisconsin Carbone Cancer Center, Madison, Wisconsin.
[4]Department of Human Oncology, University of Wisconsin–Madison, Madison, Wisconsin.

Address correspondence to: Joseph Grudzinski; Department of Medical Physics, University of Wisconsin–Madison; 1005 WI Institute Medical Research, 1111 Highland Avenue, #1005 Madison, WI 53705
E-mail: **grudzinski@wisc.edu**

localized, TNBC represents a clinical challenge because it is associated with a higher risk of relapse and poorer survival compared to other breast cancer subtypes.[4]

Inferior outcomes of clinically localized TNBC are, in large part, attributable to (a) the common presence of micrometastatic disease at diagnosis and (b) the absence of efficacious, molecularly targeted therapies such as the antiestrogenic aromatase inhibitors for ER+ breast cancer and the HER-2-directed agents such as trastuzumab for HER-2+ breast cancer.[5] The presence of micrometastases at diagnosis is a negative prognostic indicator for TNBC that portends higher rates of recurrence and death.[6] The therapies currently used to treat clinically occult TNBC micrometastatic disease are limited to conventional cytotoxic chemotherapies (e.g., anthracyclines, taxanes) that possess modest activity.[7] Therefore, there is an unmet medical need for effective treatment options that can target and destroy micrometastatic disease in TNBC patients. An agent that effectively targets and treats these micrometastases will improve the outcome of patients with TNBC. The ideal therapeutic for this setting would demonstrate cancer selectivity and a broad anticancer mechanism to address the diverse molecular lesions observed in TNBC, yet, be less toxic to normal tissue than current standard-of-care chemotherapies.

Snyder and Wood, and Snyder et al. proposed that the overabundance of ether lipids in tumors arose as a result of a lower capacity of tumor cells to metabolize these lipids.[8,9] The hypothesis that tumor cells have less ''alkyl cleavage enzyme'' activity than normal cells was exploited by Counsel et al. through the synthesis and evaluation of a series of over 30 radio-iodinated phospholipid ether (PLE) analogs as potential tumor selective imaging agents.[10,11] After basic investigation into structure–activity relationships of an array of PLE and alkylphosphocholine analogs, CLR1404 [18-(p-iodophenyl) octadecylphosphocholine] was identified as a potentially optimal cancer-specific agent (Fig. 1).

When the aromatic iodine (''X'' in Fig. 1) is substituted with fluorophores, BODIPY (CLR1501) and IR-775 (CLR1502), a very high degree of *in vitro* and *in vivo* tumor selectivity in TNBC models is retained.[12–14] CLR1501 distributes to the cell membrane and perinuclear organelles with no apparent uptake in the nucleus. The selective uptake and prolonged retention of antitumor alkyl-phospholipids has been attributed to the selective insertion of these types of compounds into distinct areas of cell membranes that contain large accumulations of sphingolipids and cholesterol known as lipid rafts.[15–19] Malignant cells have been demonstrated to have greatly increased amounts (6—10×) of membrane lipid rafts compared to normal cells[20–22] and the selective uptake and prolonged retention of CLR1404 in malignant cells compared to normal cells has been demonstrated.[12]

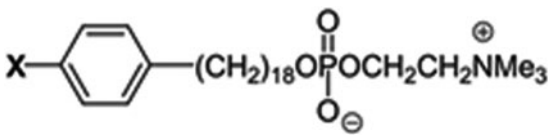

FIG. 1. Structure of alkyl-phosphocholine analog CLR1404 [18-(p-iodophenyl) octadecylphosphocholine]. CLR1404 can be synthesized as different isosteres as either chemotherapeutic (X = ^{127}I) or radioactive iodine isotopes for PET imaging (X = ^{124}I) or radiotherapy (X = ^{131}I or X = ^{125}I). PET, positron emission tomography.

In summary, the findings, combined with extensive studies in literature, support that preferential uptake of PLE analogs, such as CLR1404, in cancer cells is attributable to lipid raft incorporation with translocation to the lipid bilayers of perinuclear organelles. CLR1404-based PLE analogs have been shown to selectively target a broad spectrum of cancer cell types and to exhibit a prolonged intracellular retention.[12] A unique property of this *diapeutic* (''theranostic'') agent is that it can serve as either a diagnostic or a radiotherapeutic agent. Several Phase I and II clinical trials evaluating the cancer imaging and therapeutic capabilities of CLR1404 are currently underway or have been completed for both ^{124}I-CLR1404 (CLR 124; NCT01898273 Phase 2 in newly diagnosed or recurrent glioblastoma was terminated, NCT01516905 malignant brain tumors is ongoing but not recruiting patients, NCT01662284 Phase 1/2 advanced solid malignancies was terminated, NCT00582283 nonsmall cell lung carcinoma is ongoing but not recruiting patients, and NCT01540513 primary and metastatic brain tumors is ongoing but not recruiting patients[23]) and ^{131}I-CLR1404 (CLR 131; NCT00925275 Phase 1 relapsed or refractory advanced solid tumors has been completed,[24] NCT01495663 Phase 1 cancer that does not respond to treatment has been completed,[25] NCT02278315 Phase 1 relapsed or refractory multiple myeloma is currently recruiting participants, and NCT02952508 relapsed or refractory select B-cell malignancies is currently recruiting participants).

Preliminary preclinical data suggest that the longer-lived isotope ^{125}I ($t_{1/2}$ = 59.4 days) optimally matches the tumor kinetics of CLR1404, whereby, maximum tumor uptake occurs around 4 days postinjection with a prolonged retention phase thereafter. This has been shown both preclinically with positron emission tomography (PET) imaging out to 10 days[26] and clinically with single-photon emission computed tomography (SPECT) imaging out to 21 days.[13] The radiobiological rationale for using iodine-125 over iodine-131 for treating TNBC micrometastases is that ^{125}I decays via the emission of a cascade of Auger electrons, which deposit energy over a mean path length in tissue well below 10 μm, resulting in a high linear energy transfer (LET) on the order of 4–26 keV/μm.[27] If deposited in close proximity to the nucleus, this large LET of ^{125}I also yields a large radiobiological effect which can increase the fraction of lethal DNA damage and limits the impact of hypoxia and cell cycle dynamics on cancer cell kill.[28] In combination, these radiation characteristics are optimal for treatment of individual cancer cells or small cell clusters. This is particularly relevant for CLR1404 given its prolonged retention and perinuclear intracellular distribution. In summary, the authors hypothesize that ^{125}I-CLR1404 (CLR 125) may be well suited for therapy of TNBC, including micrometastases, due to advantageous radiobiological and physical properties.

The aim of this work was to investigate the potential of CLR 125 as a targeted radiotherapy agent for both subcutaneous xenograft and metastatic TNBC models.

Materials and Methods

Chemistry

Synthesis of 18-(p-iodophenyl)octadecyl phosphocholine was carried out as previously reported.[11] Previous physicochemical characterization of CLR1404 has shown an acid

dissociation constant *pKa* of 1.28, meaning that above pH 1.28, the compound is zwitterionic, which has been shown to be an advantageous molecular property for improving the signal-to-background ratios in diagnostic and therapeutic applications.[29,30] CLR 125 was synthesized *via* isotope exchange reaction[31] that typically affords specific activities of 2.775 GBq/μmol. ^{125}I was obtained from McMaster University. Once purified from the reaction mixture, the radioconjugate fraction was measured for activity in a Capintec dose calibrator. A sample then underwent high-performance liquid chromatography (HPLC) analysis and was compared to an analytical reference standard of the ^{127}I stable isotope labeled CLR1404. Retention time and diode array spectral analysis were used to establish identity of the isolated CLR 125. A radio detector signal confirmed that the isolated fraction consisted of radiolabeled CLR 125. The fraction containing radiolabeled CLR 125 was formulated (standard formulation in 0.4% polysorbate 20 and 0.2% ascorbic acid in saline) in a biosafety cabinet and sterile filtered through a 0.22 μm filter into an appropriate volume sterile vial. Final product analysis was performed using an Agilent 1100 HPLC equipped with a diode array detector and a LabLogic Gamma-RAM radio detector. Radiochemical identity, radiochemical purity, total mass dose, impurities and/or degradants (area percent), chemical identity by spectral comparison and retention time, specific concentration, specific activity, and pH were evaluated. The final product was found to have no detectable endotoxins at release and had no microbiota growth in medium observed for 14 days following inoculation. Preliminary stability, which was also evaluated by HPLC, was assessed out to 14 days.

Tumor models

For all efficacy studies, female nude (nu/nu) mice (20–25 g, 6–8 weeks old) were purchased from Envigo (Indianapolis, IN). Animals were housed in a temperature (20°C–-24°C), humidity (30%–70%), and light (12-hour light/dark) controlled room and given *ad libitum* access to food (No. 2018C; Harlan Teklad) and water. Tumor models were established using the luciferase expressing cell line MDA-MB-231-luc-D3H2LN (PerkinElmer), derived from MDA-MB-231 human adenocarcinoma cells. This cell line produces metastases to clinically relevant tissues such as lymph nodes, lung, and bone and permits sensitive *in vivo* detection of both primary and secondary tumor sites by bioluminescent imaging.[32] Cells were maintained in Dulbecco's modified Eagle's medium supplemented with 10% fetal bovine serum and 1% PenStrep (Gibco-BRL, Life Technologies, NY) and incubated at 37°C with 5% CO_2 in air.

To establish orthotopic xenograft TNBC tumor models, mice were injected orthotopically into the mammary fat pad with 2×10^6 cells suspended in 100 μL phosphate-buffered saline (PBS) to establish primary tumors. Metastatic TNBC tumor models were established by injecting mice intravenously with 1×10^6 MDA-MB-231-luc-D3H2LN cells suspended in 100 μL sterile Dulbecco's PBS.

Three-dimensional CLR 125 dosimetry

Internal validation has been performed to confirm that even at masses, doses of 500 times the anticipated imaging dose (CLR 124), the pharmacokinetics (PK) and biodistribution of the blood, and plasma and organs of interest are not perturbed (study not published). This confirms that CLR 124 can be used a PET imaging surrogate to estimate CLR 125 dosimetry. A Monte Carlo (MC)-based dosimetry assessment platform was used to calculate preclinical dose distributions in mouse-specific anatomy: Pseudodynamic PET/computed tomography (CT) images of mice bearing MDA-MB-231 xenografts injected with CLR 124 were acquired at 0, 24, 48, 96, 120, and 144 h postinjection to produce a four-dimensional PK profile of CLR1404. The data were then imported into an in-house MC dosimetry platform[33–35] and corrected for physical decay differences to provide mouse-specific dose estimates for the therapeutic agent CLR 125.

PET/CT imaging was performed using the Inveon micro-PET/CT (Siemens, Nashville, TN) under imaging protocols approved by the University of Wisconsin's Institutional Animal Care and Use Committee (IACUC). Details of the imaging protocol are described elsewhere.[26] In brief, mice were injected with $\sim$7.4 MBq (200 μL) of CLR 124 with a specific activity of 1.85 ± 0.74 GBq/μmol via the tail vein. Following acquisition, preprocessing of the image data and contouring of the tumors and normal tissues was performed. CLR 124 activity concentration was converted to CLR 125 uptake at each time point by correcting for the difference in physical decay rates. CT and the PET images were used in the MC simulation to define the geometry and the source distribution, respectively. After computing the cumulative activity for each PET voxel, the volume was imported into the MC framework (Geant4 version 9.6) and used as source terms in the simulation. To generate the simulation geometry, CT volume data consisting of Hounsfield units (HU) were transformed into mass density by applying the HU-to-density CT scanner specific calibration curve. Using libraries from the ENDSF (Evaluated Nuclear Structure Data File) database (Brookhaven National Laboratory) which includes all β and γ radiation emitted per decay, each source decay was sampled uniformly throughout each voxel and the energy deposition was tracked to create a three-dimensional (3D) cumulative dose distribution.

CT-based contours of the tumor and normal organs of interest were used to quantify the *in vivo* concentration of CLR 124 over time (PK) and describe the spatial distribution of the absorbed dose imparted by CLR 125 (dosimetry).

Efficacy studies

Dose escalation study. The aim of this study was to investigate the potential toxicity of CLR 125 and determine the maximum tolerable dose (MTD). To this end, 30 naive female nude mice were injected with varying doses of CLR 125 (14.8, 29.6, 44.4 and 74 MBq) or administered control vehicle injections whose mass dose was equal to the 74 MBq treatment group. These dose levels were chosen based on in-house studies of CLR1404 and dosimetry extrapolation. Mice were weighed biweekly for 90 days postinjection to assess possible toxicity from CLR 125 and were euthanized if they experienced 15% body weight loss for 3 consecutive days or 20% body weight loss for 1 day as per the IACUC protocol. All mice receiving radioiodinated CLR1404 received drinking water containing 0.1% potassium iodide supplemented with 0.4% aspartame to block the thyroid from 3 days pre- to 14 days postadministration.

Orthotopic xenograft study. The aim of this study was to determine if CLR 125 would inhibit the growth of xenograft tumors and whether that inhibition was dose dependent. Female nude mice ($n=24$) with orthotopic xenograft tumors of 3–4 mm ($\sim$2 weeks after inoculation) diameters were injected with a single intravenous dose of CLR 125 or an equivalent amount of ^{127}I-CLR1401 (three groups of $n=8$). Tumor sizes were chosen to be small enough to mimic a clinically occult human metastasis but large enough to be accurately palpable and established. The equivalent molar amount of CLR1404 was calculated using the specific molar activity of the highest CLR 125 dose. The treatment groups were injected with 44.4 or 74 MBq of CLR 125. Tumors were measured weekly using high-resolution calipers until they reached 2500 mm^3 or 60 days. To minimize interuser variability, the same researcher (blinded to the treatment group information) measured tumor volumes. The overall survival was characterized using Kaplan–Meier curves, and comparison was performed using the log-rank test. Mice were euthanized when the tumor volume was >2500 mm^3, they experienced 15% body weight loss for 3 consecutive days, or they experienced 20% body weight loss for 1 day as per the IACUC protocol.

Lung metastasis study. The aim of this study was to determine if CLR 125 would inhibit the growth of metastases from TNBC. At the time of inoculation, female nude (nu/nu) mice were injected intravenously via the tail vein with TNBC cells. On the day of imaging, mice were anesthetized and placed supine in the IVIS™ Imaging System and imaged from the ventral view approximately 15–17 min after intraperitoneal injection of 150 mg/kg of D-luciferin in water (Invitrogen, Carlsbad, CA) which was determined to yield the most signal. Imaging acquisitions lasted up to 3 min. Only mice with evidence of lung metastases continued in the experiment and were randomized into treatment or control groups (eight per group). Experimental details of when the mice are imaged and treated are outlined in Figure 2. Mice in the treatment group were administered a single intravenous injection of 74 MBq (200 μL) of CLR 125 and the control group received an equivalent mass dose of ^{127}I-CLR1401 (200 μL).

Lung metastatic burden was quantified weekly by *in vivo* bioluminescence using total photon flux as a surrogate. Using Living Image® software (Xenogen), a rectangular (2×3 cm) region of interest that encompassed the lungs was drawn and used to quantify total flux photons/second (p/s) (Fig. 2). Total photon flux with respect to time was plotted for each treatment group. Mice were euthanized if they experienced 15% body weight loss for 3 consecutive days or 20% body weight loss for 1 day as per the IACUC protocol. Measurement of photon flux has been validated to correlate with both tumor cell number and volume.[36,37]

Statistical analyses. Longitudinal data were represented using mean (±standard deviation [SD]) and analyzed using repeated measures two-way analysis of variance with *post hoc* Tukey's test. Survival analysis was performed using the Kaplan–Meier curve and log-rank test. ***$p<0.001$, **$p<0.01$, and *$p<0.05$. All statistical analyses were performed using GraphPad Prism version 7.00 for Windows (GraphPad Software, La Jolla, CA).

Results

Three-dimensional CLR 125 dosimetry

The results from estimating CLR 125 dosimetry using longitudinal CLR 124 microPET/CT imaging are shown for organs of interest and tumor in Figure 3. PET-based PK analysis showed consistent tumor uptake and retention throughout the study (4.40% ± 0.41% injecting dose per gram at 144 h), while the highly perfused tissues that is, kidney, lungs, heart (blood), and liver exhibited a rapid clearance in the distribution phase but a prolonged terminal phase. The larger concentration within the left femur bone marrow (Lt femur BM) compared with the right femur bone marrow (Rt femur BM), 2.01 ± 0.26 versus 1.06 ± 0.14 at 144 h, is most likely due to spill in from the tumor caused by partial volume effects. Consistent with the PK results, the dosimetry analysis showed that the tumor has the largest absorbed dose per injected activity (0.261 ± 0.023 Gy/MBq) while the ''Rt femur BM,'' which is generally the dose-limiting organ for CLR1404, appears to have the lowest (0.063 ± 0.005 Gy/MBq). ''Lt femur BM'' appears to have a larger dose compared with ''Rt femur BM,'' which is consistent with the PK results. Due to the prolonged retention within the blood of CLR1404, the lungs and heart have the largest doses compared to the other normal organs analyzed. These results provided a dosimetric foundation for subsequent maximum dose finding and efficacy studies. Because the MC radiation transport simulations are performed on the voxel level, they have the potential of contributing to accurate dose–response relationships for CLR 125 in TNBC.

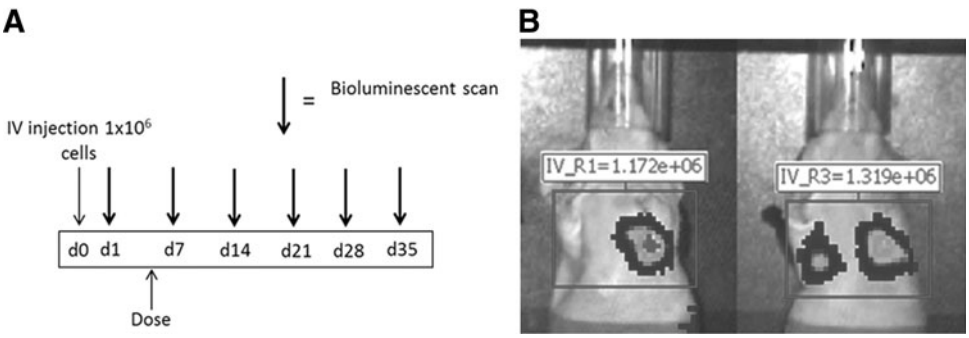

FIG. 2. **(A)** Bioluminescence imaging schedules for mice injected intravenously. with MDA-MB-231-luc-D3H2LN cells to investigate the efficacy of CLR 125 for a metastasis model. **(B)** Illustrates how the bioluminescence emitting from the lung metastases was quantified.

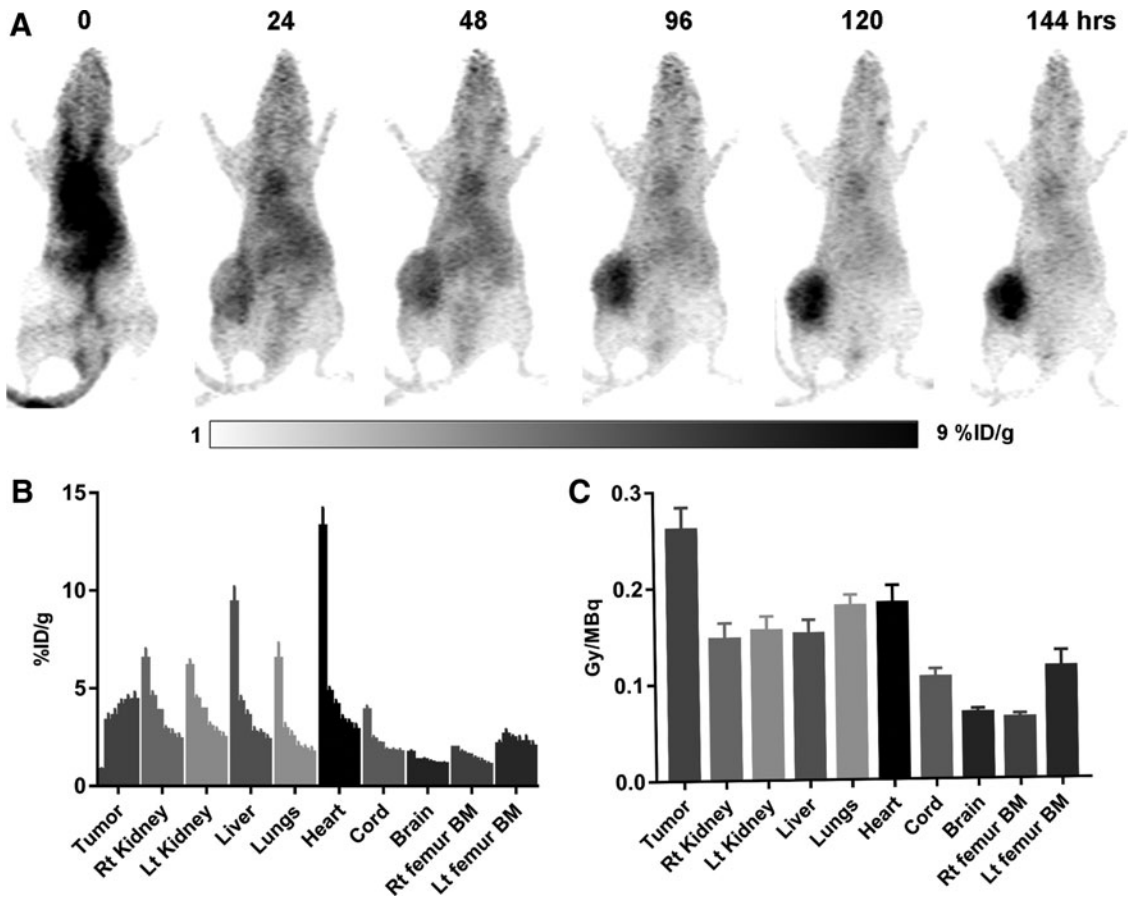

FIG. 3. PK and dosimetric results of CLR 124/125 for mice bearing orthotopic MDA-MB-231 tumors. **(A)** MIP of a decay-corrected imaging series of a representative mouse injected with CLR 124 and microPET/CT imaged at 0, 24, 48, 96, 120, and 144 h postinjection. **(B)** Summary results from the PK analysis showing the mean (±SD) concentration (percent ID/g) of CLR 124 within each ROI over time, **(C)** Summary results from the dosimetry analysis showing the mean (±SD) absorbed dose (Gy/MBq) of CLR 125 within each ROI. Consistent with the PK results, the dosimetry analysis showed that the tumor has the largest absorbed dose per injected activity while the ''Rt femur BM,'' which is generally the dose-limiting organ for CLR1404, appears to have the lowest. ''Lt femur BM'' appears to have a larger dose compared to ''Rt femur BM'' which is consistent with the PK results. Due to the prolonged retention within the blood of CLR1404, the lungs and heart have the largest doses compared to the other normal organs analyzed. CT, computed tomography; ID, injecting dose; Lt femur BM, left femur bone marrow; MIP, maximum intensity projections; PK, pharmacokinetic; ROI, region of interest; Rt femur BM, right femur bone marrow; SD, standard deviation.

Efficacy studies

MTD study. The mean (±D) animal weights of each dose groups are shown in Figure 4. There is no significant difference between any two of the dose groups ($p > 0.05$). Although the results of the MTD study do not determine a definitive MTD, they do show that the proposed radioactivity levels to be used would be safe for use in subsequent efficacy studies. No mice were euthanized due to weight loss.

Orthotopic xenograft. Tumor volume measurements and Kaplan–Meier survival analysis data are shown in Figure 5. From these results, it is evident that CLR 125 has caused a considerable reduction in tumor volume compared with the control group at day 60 ($\sim$60% reduction in volume). In addition, all the mice that were injected with 74 MBq of CLR 125, which amounted to an approximate tumor dose of 19 Gy according to the previous dosimetry analysis, survived past 60 days while all but two survived for the 44.4 MBq dose group. Only 25% of the control group survived past day 60. Based on the Kaplan–Meier survival curves, it is evident that CLR 125 improved survival. However, according to the log-rank test between cohorts, the survival difference between the control group and 74 MBq group was the only statistically significant ($p < 0.05$) comparison.

Lung metastases. The results from the metastasis study are presented in Figure 6. It appears that lung metastases start to form after 3 weeks. At day 28, 74 MBq of CLR 125 starts to affect the progression of lung metastases but not statistically significantly. Statistical significance is achieved at day 35 where 74 MBq of CLR 125 reduces the progression of TNBC metastases compared with the control group.

Discussion

The authors have investigated a novel Auger electron-emitting targeted radiotherapeutic (TRT) agent against TNBC.

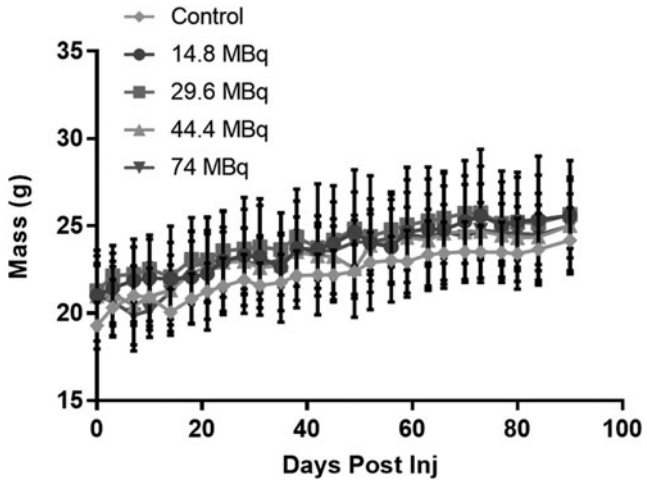

FIG. 4. The average mass (±SD) within each dose group is plotted over time. There is a not a significant difference between any two of the dose groups ($p > 0.05$), repeated measures two-way ANOVA with Tukey's *ad hoc* test. ANOVA, analysis of variance.

Furthermore, CLR 124 PET imaging supports the assumption that CLR 125 targets TNBC *in vivo* and possesses prolonged retention that is corroborated by excellent antitumor efficacy *in vivo* in mice bearing both orthotopic TNBC xenografts ($p < 0.001$) and lung metastases ($p < 0.05$). This is one of the few studies to demonstrate antitumor efficacy after systemic administration of an Auger TRT agent[38–41] and the only study to the authors' knowledge that uses bioluminescence imaging of metastases to investigate efficacy. Although β emitters are likely to remain more effective for treatment of macroscopic disease, Auger emitters are recognized to have potential advantages for treatment of micrometastatic cancer, including higher LET and much shorter range than β emitters or X-rays.[42–46] The potential for Auger emitter therapy was confirmed by the results demonstrating a reduction of tumor volume. Although the focus of this work was to test the efficacy of CLR 125 against metastases, which should be advantageous for Auger emitters such as CLR 125, the results of the orthotopic xenograft study provided support for the cytotoxic nature of CLR 125 against cancer cells even though β-emitting radioisotopes may have been more effective against these relatively large tumors. In addition, the establishment of the orthotopic xenograft model aided us in quantitatively measuring the uptake distribution of CLR 125 via CLR 124 microPET/CT and provided us with quantitative 3D data for estimating dosimetry and establishing dose–response relationships. The heterogeneity of the CLR 124 combined with the local deposition of CLR 125 (illustrated in Fig. 3) further reiterates that CLR 125 may be more effective against metastases than larger tumors. However, the high uptake and prolonged retention of CLR 125, substantiated by CLR 124 microPET/CT imaging in this study and PET and SPECT imaging in past studies, provide evidence that the long physical half-life of ^{125}I (59.4 days) allows CLR 125 to sustain tumor therapy by continuous exposure resulting in DNA damage to TNBC. In addition, the dose-escalation study showed no animal deaths, weight loss, or other signs of toxicity at any dose up to 74 MBq at the time points assessed.

Even though high-resolution calipers are the most widely used and accepted tool for measuring tumor volumes in drug efficacy studies, researchers argue that sometimes measurements are not reproducible and are prone to bias. To alleviate these concerns, researchers are starting to adapt more sophisticated and ''quantitative'' measurement tools such as CT or bioluminescence imaging. Although CT has the advantage of being able to produce high-resolution volumetric results, it suffers from poor soft tissue contrast so that nonviable tissue such as areas of necrosis are difficult to discern and are incorrectly counted as viable tumor tissue. In contrast, bioluminescence imaging has the advantage of imaging only the viable tumor cells. However, due to limitations of near infrared imaging such as poor tissue penetration and photon absorption and scattering, true ''quantitative'' optical imaging is very difficult especially when imaging a xenograft tumor because the tissue heterogeneity and changing volume increase the quantitative uncertainty. Studies aimed at imaging thinner tissues such as metastases should possess less uncertainty.

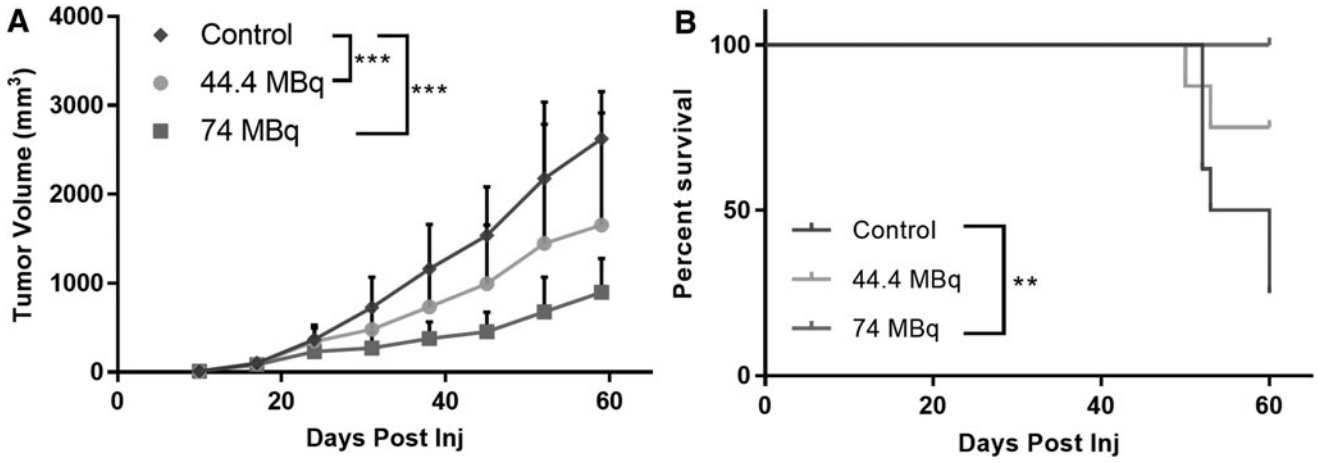

FIG. 5. The mean tumor volume (mm^3; ±SD) **(A)** and Kaplan–Meier survival **(B)** after administration of CLR 125 or control. The data in **(A, B)** were statistically analyzed with a repeated measures two-way ANOVA with Tukey's *ad hoc* test and log-rank test, respectively, $***p < 0.001$, $**p < 0.01$.

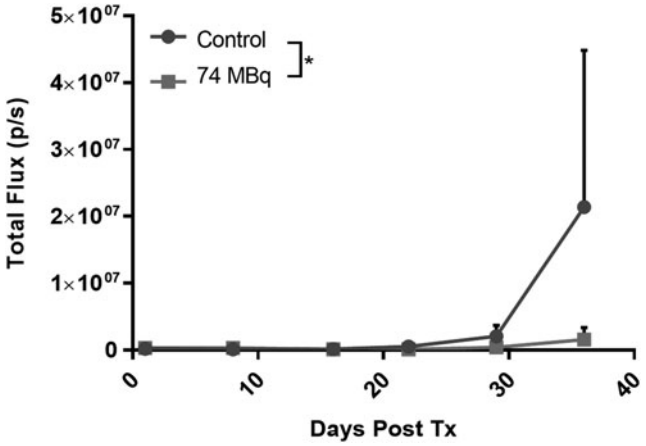

FIG. 6. *In vivo* bioluminescence imaging results for the metastasis study. The figure shows the weekly mean signal (p/s; ±SD), which is proportional to metastatic progression, after administration of CLR 125. p/s, photons/second.

With the short range of Auger electrons, a major challenge is to achieve proximity to DNA to cause strand breaks. Using confocal microscopy with a fluorescent analog of CLR1404, CLR1501,[12] the authors have previously shown that this agent localizes not only in the plasma membrane but also to the perinuclear organelles. The discrete perinuclear foci that are observed are consistent with localization to the mitotic spindle poles, which would bring the Auger emitter close to DNA during mitosis, especially in anaphase when the condensed chromosomes are pulled toward the spindle poles.[47] Proximity is critical for direct DNA damage because, although ^{125}I emits ~20 Auger electrons per decay, most of these have a range of less than 10 μm.[48] This provides an additional layer of cancer specificity for CLR 125, as the close vicinity between the spindle poles and chromosomes would occur only in actively dividing tumors.

Studies have shown that ^{125}I exposure to normal cells does not appear to cause harm, and exposure to weak iodine X-rays perhaps would not be of major concern when treating patients with large doses of ^{125}I. The relative inefficiency of the Auger electron emitter ^{125}I for cell killing when the radionuclide is located in the cytoplasm or outside the cell makes ^{125}I superior to other high-energy radionuclides by reducing the potential toxicity to nontarget cells.[49] This may effectively spare the bone marrow and blood cells leading to less than expected hematologic toxicity. In this study, mice did not experience any signs of toxicity after being administered 74 MBq of CLR 125, which equates to a human equivalent dose of 22.2 GBq.

Despite positive preclinical efficacy data in many cancer models found in the literature, ^{125}I has been limited clinically as a systemically administered TRT and has not advanced past Phase II clinical trials.[28,50–54] In clinical trials, it has been difficult to reach a MTD for certain agents even at large doses of ^{125}I (several hundred millicuries), which was like what was seen in the study. The projected MTD, estimated with dosimetric modeling, could cause occupational radiation safety concerns because clinics are not equipped to handle patients with such substantial amounts of radiopharmaceutical onboard, and could be further complicated if the agent is cleared renally. Combined with the long half-life, the use of ^{125}I is currently logistically challenging. However, as more TRTs become commercially available and clinics adapt to this change, it may be beneficial to revisit the long-lived TRTs that have stalled clinically. Viable solutions to improve clinical translation of long-lived TRT agents are a paradigm shift in clinical trial design, implementing patient-specific prescriptions, and combination with conventional therapies. Instead of trying to find the MTD of a drug, it may be more ideal for a TRT agent to find the dose that causes the biological effect, or biologically effective dose (BED). MTD studies are based around finding the maximum tolerable radioactivity per body mass or surface area while BED studies focus on the biological effect caused by the radiation imparted on the body. BED studies aim to establish dose–response relationships which help correlate radiation dosimetry to changes in biological parameters. In addition, BED studies are better optimized using patient-specific prescriptions of TRT doses to maximize the chance of efficacy while minimizing toxicity. MTD studies, in contrast, prescribed TRT doses on a population level, which unfortunately leads to possible under- and overdosing. Finally, more research has to be done with the combination of TRT agents with other therapies. Inevitably, TRT has many challenges as a monotherapy for solid tumors but could prove advantageous as a neoadjuvant therapy against disseminated disease. In addition, the innate low-dose rate and targeted nature of TRT could prove to have synergistic benefits when combined with conventional first-line therapies.

TNBC represents a pressing unmet medical need due, in large part, to a lack of efficacious targeted therapies that serve as a cornerstone of treatment for other breast cancer subtypes. Treatment of TNBC may benefit from leveraging tumor targeting mechanisms that are more ubiquitous, such as iodinated PLEs. CLR1404 is an interesting APC platform whose ''bulk tolerance'' allows for multiscaled and multimodality optimization of TRTs. For example, information gleaned from the optical and PET analogs of CLR1404 can be leveraged for not only research and development but also potential personalized medicine approaches. Based on the preclinical results presented, CLR 125 is an intriguing agent possibly worthy of further development, despite past difficulties with other ^{125}I TRTs.

Conclusions

Lipid raft-targeted radionuclide therapy with the Auger electron emitter CLR 125 yielded specific TNBC cell kill in both primary xenografts and lung metastases after systemic administration, showing promise for treatment of TNBC. Given prolonged plasma retention of CLR1404 demonstrated clinically in Phase I trials, long-term hematological toxicity and dosimetry studies are warranted to assess safety for further translation of CLR 125.

Ethical Approval

All procedures involving animals were approved by the University of Wisconsin's IACUC. The studies that were conducted did not involve human subjects.

Acknowledgments

This project has been funded in whole or in part with Federal funds from the National Cancer Institute, National

Institutes of Health, Department of Health and Human Services, under Contract No. HHSN261201500071C.

Authors' Contributions

J.G., B.T., and K.K. designed the experiments while J.G., J.L., A.W., and J.J. executed them. M.L. and K.L. manufactured CLR 125 and analyzed it. A.M. created the animal models and assisted with animal studies while I.M. and B.B. performed image processing and radiation simulations. J.G. wrote the article with consultation from the other authors.

Disclosure Statement

Authors J.G., B.T., M.L., K.K., K.L., and J.L. were all employed by Cellectar Biosciences when this work was conducted. All other authors declare that they have no conflict of interest.

References

1. Edwards BK, Noone A-M, Mariotto AB, et al. Annual Report to the Nation on the status of cancer, 1975–2010, featuring prevalence of comorbidity and impact on survival among persons with lung, colorectal, breast, or prostate cancer. Cancer 2014;120:1290.
2. DeSantis C, Siegel R, Bandi P, et al. Breast cancer statistics, 2011. CA Cancer J Clin 2011;61:409.
3. Giltnane JM, Balko JM. Rationale for targeting the Ras/MAPK pathway in triple-negative breast cancer. Discov Med 2014;17:275.
4. Keam B, Im S-A, Kim H-J, et al. Prognostic impact of clinicopathologic parameters in stage II/III breast cancer treated with neoadjuvant docetaxel and doxorubicin chemotherapy: Paradoxical features of the triple negative breast cancer. BMC Cancer 2007;7:203.
5. Boyle P. Triple-negative breast cancer: Epidemiological considerations and recommendations. Ann Oncol 2012;23:8.
6. Castellano I, Allia E, Accortanzo V, et al. Androgen receptor expression is a significant prognostic factor in estrogen receptor positive breast cancers. Breast Cancer Res Treat 2010;124:607.
7. Hudis CA, Gianni L. Triple-negative breast cancer: An unmet medical need. Oncologist 2011;16(suppl1):1.
8. Snyder F, Wood R. The occurrence and metabolism of alkyl and alk-1-enyl ethers of glycerol in transplantable rat and mouse tumors. Cancer Res 1968;28:972.
9. Snyder F, Blank ML, Morris HP. Occurrence and nature of O-alkyl and O-alk-I-enyl moieties of glycerol in lipids of Morris transplanted hepatomas and normal rat liver. Biochim Biophys Acta 1969;176:502.
10. Counsell RE, Longino MA, Pinchuk AN, et al. Radioiodinated phospholipid ethers and analogs as tumor imaging agents. Fourth International Symposium on Radiohalogens, Whistler, September 9–13, 2000:33.
11. Pinchuk AN, Rampy MA, Longino MA, et al. Synthesis and structure-activity relationship effects on the tumor avidity of radioiodinated phospholipid ether analogues. J Med Chem 2006;49:2155.
12. Weichert JP, Clark PA, Kandela IK, et al. Alkylphosphocholine analogs for broad-spectrum cancer imaging and therapy. Sci Transl Med 2014;6:240ra75.
13. Deming DA, Maher ME, Leystra AA, et al. Phospholipid ether analogs for the detection of colorectal tumors. PloS One 2014;9:e109668.
14. Korb ML, Warram JM, Grudzinski J, et al. Breast cancer imaging using the near-infrared fluorescent. Mol Imaging 2014;13:1.
15. Kirschner AS, Ice RD, Beierwaltes WH. Radiation dosimetry of 131I-19-iodocholesterol. J Nucl Med 1973;14:713.
16. Carrasco MP, Jiménez-López JM, Ríos-Marco P, et al. Disruption of cellular cholesterol transport and homeostasis as a novel mechanism of action of membrane-targeted alkylphospholipid analogues. Br J Pharmacol 2010;160:355.
17. Gajate C. The antitumor ether lipid ET-18-OCH3 induces apoptosis through translocation and capping of Fas/CD95 into membrane rafts in human leukemic cells. Blood 2001;98:3860.
18. Reis-Sobreiro M, Roué G, Moros a, et al. Lipid raft-mediated Akt signaling as a therapeutic target in mantle cell lymphoma. Blood Cancer J 2013;3:e118.
19. van der Luit AH, Budde M, Ruurs P, et al. Alkyl-lysophospholipid accumulates in lipid rafts and induces apoptosis via raft-dependent endocytosis and inhibition of phosphatidylcholine synthesis. J Biol Chem 2002;277:39541.
20. Lasserre R, Guo X-J, Conchonaud F, et al. Raft nanodomains contribute to Akt/PKB plasma membrane recruitment and activation. Nat Chem Biol 2008;4:538.
21. Li YC, Park MJ, Ye S-K, et al. Elevated levels of cholesterol-rich lipid rafts in cancer cells are correlated with apoptosis sensitivity induced by cholesterol-depleting agents. Am J Pathol 2006;168:1107.
22. Mollinedo F, Gajate C. Lipid rafts and clusters of apoptotic signaling molecule-enriched rafts in cancer therapy. Future Oncol 2010;6:811.
23. Hall LT, Titz B, Robins HI, et al. I-CLR1404 in high and low-grade brain tumors. Am J Nucl Med Mol Imaging 2017;7:157.
24. Grudzinski JJ, Titz B, Kozak K, et al. A phase 1 study of 131I-CLR1404 in patients with relapsed or refractory advanced solid tumors: dosimetry, biodistribution, pharmacokinetics, and safety. Doherty TM, editor. PLoS One Public Library of Science; 2014;9:e111652.
25. Lubner SJ, Mullvain J, Perlman S, et al. A phase 1, multicenter, open-label, dose-escalation study of I-CLR1404 in subjects with relapsed or refractory advanced solid malignancies I-CLR1404 in subjects with relapsed or refractory advanced solid malignancies. Cancer Invest 2015;33:483.
26. Grudzinski JJ, Floberg JM, Mudd SR, et al. Application of a whole-body pharmacokinetic model for targeted radionuclide therapy to NM404 and FLT. Phys Med Biol 2012;57:1641.
27. Bodei L, Kassis AI, Adelstein SJ, et al. Radionuclide therapy with iodine-125 and other auger-electron-emitting radionuclides: Experimental models and clinical applications. Cancer Biother Radiopharm 2003;18:861.
28. Welt S, Scott a M, Divgi CR, et al. Phase I/II study of iodine 125-labeled monoclonal antibody A33 in patients with advanced colon cancer. J Clin Oncol 1996;14:1787.
29. Choi HS, Nasr K, Alyabyev S, et al. Synthesis and in vivo fate of zwitterionic near-infrared fluorophores. Angew Chem Int Ed Engl 2011;50:6258.
30. Choi HS, Gibbs SL, Lee JH, et al. Targeted zwitterionic near-infrared fluorophores for improved optical imaging. Nat Biotechnol 2013;31:148.
31. Mangner TJ, Wu JL, Wieland DM. Solid-phase exchange radioiodination of aryl iodides. Facilitation by ammonium sulfate. J Org Chem 1982;47:1484.
32. Jenkins DE, Hornig YS, Oei Y, et al. Bioluminescent human breast cancer cell lines that permit rapid and sensitive in vivo

detection of mammary tumors and multiple metastases in immune deficient mice. Breast Cancer Res 2005;7:R444.
33. Besemer A, Bednarz B. SU-E-T-345: Validation of a patient-specific Monte Carlo targeted radionuclide therapy dosimetry platform. Med Phys 2014;41:303.
34. Besemer A, Grudzinski J, Titz B, et al. SU-F-500-01: Towards personalized dosimetry using diapeutic radiopharmaceuticals. Med Phys 2013;40:382.
35. Bednarz B, Grudzinski J, Titz B, et al. Monte Carlo-based radiation dosimetry for preclinical trials of radiohalogenated pharmaceuticals. Transact Am Nucl Soc 2013;108:43.
36. Hickson J, Ackler S, Klaubert D, et al. Noninvasive molecular imaging of apoptosis in vivo using a modified firefly luciferase substrate, Z-DEVD-aminoluciferin. Cell Death Differ 2010;17:1003.
37. Adiseshaiah PP, Patel NL, Ileva LV, et al. Longitudinal imaging of cancer cell metastases in two preclinical models: A correlation of noninvasive imaging to histopathology. Int J Mol Imaging 2014;2014:102702.
38. Michel RB, Rosario AV, Andrews PM, et al. Therapy of small subcutaneous B-lymphoma xenografts with antibodies conjugated to radionuclides emitting low-energy electrons. Clin Cancer Res 2005;11:777.
39. Barendswaard EC, Humm JL, O'Donoghue JA, et al. Relative therapeutic efficacy of (125)I- and (131)I-labeled monoclonal antibody A33 in a human colon cancer xenograft. J Nucl Med 2001;42:1251.
40. Santoro L, Boutaleb S, Garambois V, et al. Non-internalizing monoclonal antibodies are suitable candidates for 125I radioimmunotherapy of small-volume peritoneal carcinomatosis. J Nucl Med 2009;50:2033.
41. Behr TM, Sgouros G, Vougiokas V, et al. Therapeutic efficacy and dose-limiting toxicity of Auger-electron vs. beta emitters in radioimmunotherapy with internalizing antibodies: Evaluation of 125I- vs. 131I-labeled CO17-1A in a human colorectal cancer model. Int J Cancer 1998;76:738.
42. Bousis C, Emfietzoglou D, Nikjoo H. Monte Carlo single-cell dosimetry of I-131, I-125 and I-123 for targeted radioimmunotherapy of B-cell lymphoma. Int J Radiat Biol 2012;88:908.
43. Behr TM, Behe M, Lohr M, et al. Therapeutic advantages of Auger electron- over beta-emitting radiometals or radioiodine when conjugated to internalizing antibodies. Eur J Nucl Med 2000;27:753.
44. Zanzonico PB. Internal radionuclide radiation dosimetry: A review of basic concepts and recent developments. J Nucl Med 2000;41:297.
45. Arnaud FX, Paillas S, Pouget JP, et al. Complex cell geometry and sources distribution model for Monte Carlo single cell dosimetry with iodine 125 radioimmunotherapy. Nucl Instrum Methods Phys Res B 2016;366:227.
46. Raisali G, Mirzakhanian L, Masoudi SF, et al. Calculation of DNA strand breaks due to direct and indirect effects of Auger electrons from incorporated 123I and 125I radionuclides using the Geant4 computer code. Int J Radiat Biol 2013;89:57–64.
47. Kiess AP, Minn I, Chen Y, et al. Auger radiopharmaceutical therapy targeting prostate-specific membrane antigen. J Nucl Med 2015;56:1401.
48. Balagurumoorthy P, Xu X, Wang K, et al. Effect of distance between decaying 125I and DNA on Auger-electron induced double-strand break yield. Int J Radiat Biol 2012;88:998.
49. Quang TS, Brady LW. Radioimmunotherapy as a novel treatment regimen: 125I-labeled monoclonal antibody 425 in the treatment of high-grade brain gliomas. Int J Radiat Oncol Biol Phys 2004;58:972.
50. Mahe MA, Fumoleau P, Fabbro M, et al. A phase II study of intraperitoneal radioimmunotherapy with iodine-131-labeled monoclonal antibody OC-125 in patients with residual ovarian carcinoma. Clin Cancer Res 1999;5:3249s.
51. Li L, Quang TS, Gracely EJ, et al. A phase II study of anti-epidermal growth factor receptor radioimmunotherapy in the treatment of glioblastoma multiforme. J Neurosurg 2010;113:192.
52. Sisson JC, Hutchinson RJ, Shapiro B, et al. Iodine-125-MIBG to treat neuroblastoma: Preliminary report. J Nucl Med 1990;31:1479.
53. Emrich JG, Brady LW, Quang TS, et al. Radioiodinated (I-125) monoclonal antibody 425 in the treatment of high grade glioma patients: Ten-year synopsis of a novel treatment. Am J Clin Oncol 2002;25:541.
54. Sisson JC, Shapiro B, Hutchinson RJ, et al. Survival of patients with neuroblastoma treated with 125-I MIBG. Am J Clin Oncol 1996;19:144.